Available online at www.sciencedirect.com

ScienceDirect

materialstoday: PROCEEDINGS

Materials Today: Proceedings 3 (2016) 816 – 824

12th International Conference on Nanosciences & Nanotechnologies & 8th International Symposium on Flexible Organic Electronics

Electronic Structure of ZnO Quantum Dots Studied by High-Frequency EPR, ESE, ENDOR and ODMR Spectroscopy

P.G. Baranov[a,b], , N.G. Romanov[a], A.P. Bundakova[a], S.B. Orlinskii[c], C. De Mello Donegá[d], J. Schmidt[e]

[a]*Ioffe Institute, Politekhnicheskaya 26, St. Petersburg, 194021 Russia*
[b]*Peter the Great St. Petersburg Polytechnic University, St. Petersburg 195251, Russia*
[c]*Federal Center of Shared Facilities, Kazan State University, Kazan, Russia*
[d]*Debye Institute for Nanomaterials Science, Utrecht University, Netherlands*
[e]*Huygens Laboratory, Leiden University, Netherlands*

Abstract

High-frequency electron paramagnetic resonance (EPR), electron spin echo (ESE), electron-nuclear double resonance (ENDOR) and optically detected magnetic resonance (ODMR) were applied for the investigation of the electronic properties of ZnO colloidal quantum dots (QDs) which consist of a ZnO nanocrystal core and $Zn(OH)_2$ shell. Shallow donors (SDs) in the form of interstitial atoms of lithium and sodium, as well as substituent of the aluminum have been identified and the spatial distribution of their electronic wave functions has been determined in the regime of quantum confinement. Hyperfine interactions as monitored by ENDOR quantitatively reveal the transition from semiconductor to molecular properties upon reduction of the size of the nanoparticles. We studied the process of charge separation in the quantum dot when excited by UV light resulting in the formation of shallow donors and deep acceptors in the paramagnetic state, which recombine when heated, accompanied by thermoluminescence go back again in the non-paramagnetic state. It was shown that in all studied quantum dots deep acceptors are present positioned near the interface and including one sodium atom. ODMR techniques, which is based on EPR detection via photoluminescence or via tunneling afterglow that can be observed after preliminary X-ray or UV irradiation proved to be very useful to study colloidal ZnO NCs. The higher sensitivity of ODMR via afterglow allowed characterization of ZnO QDs dispersed in transparent media, which is an important advantage, since these systems are more relevant for a number of practical applications. A direct evidence of Co (Mn) interaction with SD in the core and hyperfine coupling with ^1H in the shell of QDs has been demonstrated in Mn (Co)-doped ZnO QDs, which are promising classes of diluted magnetic semiconductors.

Selection and peer-review under responsibility of the Conference Committee Members of NANOTEXNOLOGY2015
(12th International Conference on Nanosciences & Nanotechnologies & 8th International Symposium on Flexible Organic Electronics)

Selection and peer-review under responsibility of the Conference Committee Members of NANOTEXNOLOGY2015 (12th International Conference on Nanosciences & Nanotechnologies & 8th International Symposium on Flexible Organic Electronics)
doi:10.1016/j.matpr.2016.02.014

Keywords: ZnO, quantum dots, colloidal nanocrystals, EPR, ESE, ENDOR, ODMR

1. Introduction

ZnO offers a unique combination of high band gap energy and the exciton stability. ZnO is an even brighter emitter than GaN, because its excitons have a 60-meV binding energy, as compared with 24 meV for GaN. ZnO quantum dots (QDs) are particularly attractive since the confinement of the electronic wave function allows the optical and electronic properties to be tuned. Doped ZnO quantum dots, which can be easily processed at temperatures much lower than those for bulk ZnO crystals, are of particular interest due to their potential use in light-emitting and photovoltaic devices (see [1,2] and references therein).

Semiconductor QDs doped with transition metal ions (diluted magnetic semiconductor quantum dots, DMS QDs) have recently drawn considerable attention due to their potential applications in spintronics. For practical spintronics applications, ferromagnetic DMSs with Curie temperatures (TC) exceeding room temperature will be required [3]. One of the most promising classes of DMSs is the wide-band-gap oxides of ZnO. Theoretical predictions of high-T_C ferromagnetism in DMSs of ZnO stimulated efforts to develop these materials. It was suggested to achieve high-T_C ferromagnetism in ZnO:Mn^{2+} and ZnO:Co^{2+} DMSs by controlling the carrier density. Transition ion-carrier exchange interactions in DMSs have been exploited to control the polarizations of carrier spins in semiconductor spintronics device structures.

A striking property of single semiconductor QDs is their blinking behavior when continuously excited with above-band-gap laser light [4]. The luminescence produced by exciton recombination is interrupted at random times and for random durations. Physical models to explain this blinking involve a separation of the electron and the hole by trapping of an electron in the matrix in which the nanocrystals are embedded [5]. For capped nanocrystals it is observed that the “on” periods are considerably longer than for uncapped nanocrystals. This phenomenon is explained by assuming that the hole is trapped in the capping layer [6].

Recently we have demonstrated that ZnO QDs can be doped with shallow, interstitial Li, Na and substitutional Al donors [7]. A prerequisite for the observation of the electron paramagnetic resonance (EPR) signal of the unpaired spin of these donors at low temperatures is that the QDs are first irradiated with above-band-gap light. This observation shows that there must be (deep) acceptors present in the QDs that capture the thermally excited donor electrons at room temperature. These electrons remain frozen at the acceptor sites when the material is cooled in the dark to low temperature. The above-band-gap light transfers the electron from the acceptor to the donor and makes both sites paramagnetic. It would be interesting to identify this deep acceptor, and to decide whether it is an intrinsic defect (vacancy, antisite or interstitial) or related to an impurity. In addition, it would be interesting to determine its position in the QD in particular whether it is located in the capping layer or at the interface between the core and the capping layer. Such identification would not only be of interest to characterize the electronic properties of the QD but would also lend considerable support to the models developed for the blinking behavior of QDs. From EPR and electron nuclear double resonance (ENDOR) experiments it is concluded that in ZnO nanocrystals a deep Na-related acceptor is located at the interface of the ZnO core and the Zn(OH)2 capping layer. In particles with radii smaller than 1.5 nm these deep acceptors form exchange-coupled pairs with shallow donors. The identification of this deep surface acceptor is considered as a support for current models to explain the blinking behavior of single II-VI QDs, in which deep surface acceptors play an essential role.

The goal of this report is to summarize the existing information about EPR and ENDOR identification of defects and carriers in ZnO QDs including impurities of Mn and Co transition ions. We present the results of an EPR, ENDOR and ODMR study on dry powders of free-standing, $Zn(OH)_2$-capped, ZnO nanocrystals doped with different types of shallow donors and magnetic impurities.

2. Experimental

In this report, we will discuss experimental results obtained on powder samples of free-standing hydroxyl-capped ZnO QDs with average radius ranging from 1.1 to 3 nm. The method was based on the hydrolysis of Zn^{2+} ions in absolute alcohols, using either $LiOH•H_2O$ for the Li-doped QDs or NaOH for the Na-doped QDs. The size of the nanocrystals was controlled by the growth duration. The average radius of the nanocrystals was estimated by X-ray powder diffraction, based on the peak broadening due to the finite crystallite sizes, and by UV-Visible absorption spectroscopy, based on the size dependence of the band gap owing to quantum-size effects and using a calibration curve [8,9]. ZnO QDs doped with Al were prepared using $Zn(Ac)_2•2H_2O$, $Al(NO_3)_2•9H_2O$ and $LiOH•H_2O$ which were separately dissolved in ethanol [10]. A transmission electron microscopy (TEM) image of a representative sample and a model of the $ZnO/Zn(OH)_2$ core–shell structure are shown in the top of Fig. 1.

The EPR and ENDOR experiments were performed at 1.6 K on a pulsed 94.9 GHz EPR/ENDOR spectrometer and on a similar system operating at 275 GHz [8]. The EPR spectra were recorded by monitoring the electron spin echo (ESE) signal following a microwave π/2- and π-pulse sequence. The ENDOR spectra were obtained by monitoring the intensity of the stimulated echo, following three microwave π/2 pulses, as a function of a radiofrequency pulse applied between the second and third microwave pulses.

ODMR at 35 and 94 GHz was recorded at 1.8-2 K by monitoring the intensity of photoluminescence or tunnelling afterglow.

3. Results and discussion

Fig. 1 shows ESE-detected EPR spectra at 94.9 GHz of a dry powder sample of ZnO QDs with a radius of 1.17 nm (a) and 3 nm (b) after continuous ultraviolet (UV) irradiation at 1.6 K.

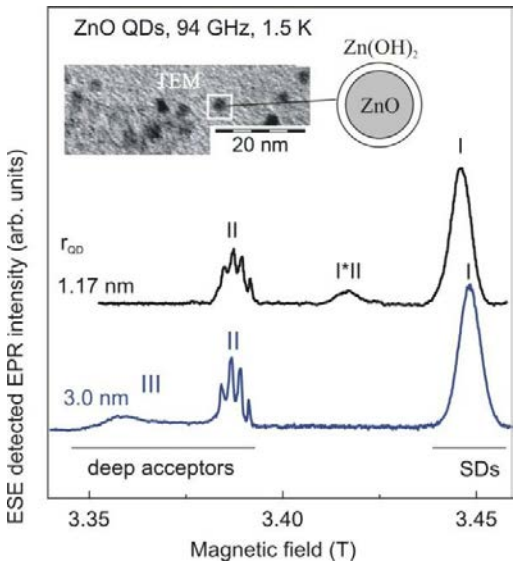

Fig. 1. The ESE-detected EPR spectrum at 94.9 GHz of a dry powder sample of Li-doped ZnO quantum dots (QDs) with an average radius of 1.17 nm and 3.0 nm recorded at 1.5 K after prolonged UV irradiation. The signals marked I are arising from shallow donors in the ZnO nanocrystal core, the signals marked II are arising from the deep Na-related surface acceptors and the signal marked III is arising from deep Zn-vacancy related acceptors in the core. The signal on exactly halfway between signal I and II marked I*II is arising from donor-acceptor pairs formed by the shallow donor (signal I) and the deep Na-related acceptor (signal II). The TEM image of ZnO nanocrystals collected from a clear solution in ethanol just after synthesis is shown in the top.

The spectra look very similar but with an important difference: for smaller radius QDs a new EPR signal marked

I*II is visible halfway between the signal of the shallow donor marked I and the signal marked II. Signal II is assigned to a deep Na-related surface acceptor. Signal I*II is attributed to an exchange-coupled donor –acceptor pair formed by the shallow donor (SD) and the deep Na acceptor.

Fig. 2 shows ESE detected ENDOR signals of the ^{67}Zn, ^{7}Li, ^{23}Na, ^{27}Al, and ^{1}H nuclear spins observed at 94.9 GHz in the EPR signal I (see Fig. 1) of the shallow donors in ZnO QDs with an average radius of 3.0 nm. The ENDOR transitions of ^{67}Zn are shown for Li-doped ZnO QDs with average radii of 1.17, 1.6 and 3.0 nm. The ENDOR transitions of ^{23}Na and ^{27}Al as observed in the EPR signal of the shallow donor in Na-doped and Al-doped ZnO QDs with an average radius of 3.0 nm. The ENDOR spectrum of ^{1}H nuclear spins of the hydrogen interstitial shallow donor in nominally pure ZnO single crystal with c axis parallel to the static magnetic field is also presented for comparison.

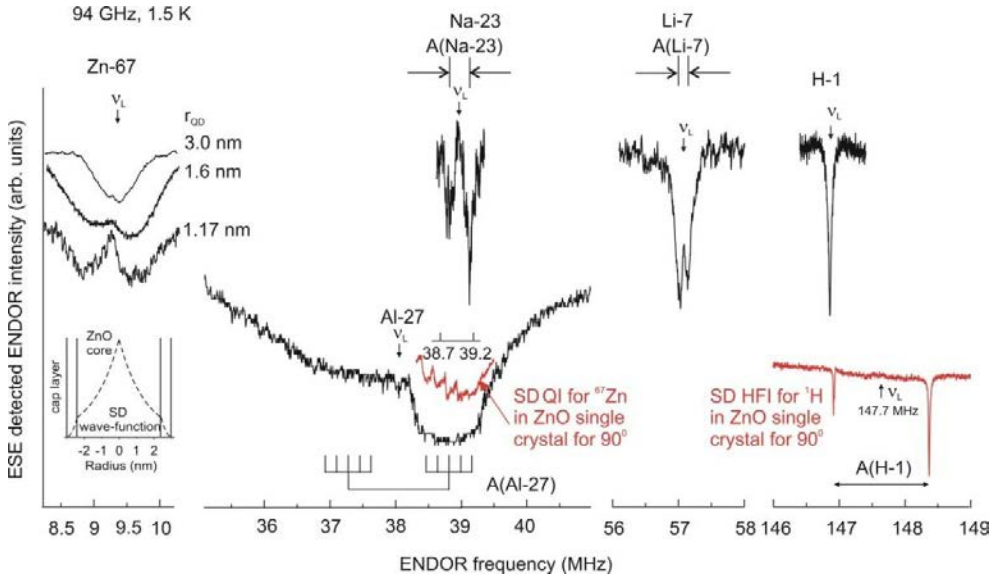

Fig. 2. The ESE detected ENDOR transitions of the ^{67}Zn, ^{7}Li, ^{23}Na, ^{27}Al, and ^{1}H nuclear spins observed at 94.9 GHz in the EPR signal I (see Fig. 1) of the shallow donors in ZnO QDs with an average radius of 3.0 nm. The ENDOR transitions of ^{67}Zn are shown for Li-doped ZnO QDs with average radii of 1.17, 1.6 and 3.0 nm. The ENDOR transitions of ^{23}Na and ^{27}Al as observed in the EPR signal of the shallow donor in Na-doped and Al-doped ZnO QDs with an average radius of 3.0 nm. The ENDOR spectrum of ^{1}H nuclear spins of the hydrogen interstitial shallow donor in nominally pure ZnO single crystal with c axis parallel to the static magnetic field is presented for comparison.

It is seen in Fig. 2 that symmetrically around the Zeeman frequency of ^{67}Zn (I = 5/2, abundance 4.1 %) at 9.2 MHz a broad, unresolved set of ENDOR lines of ^{67}Zn spins is present. From the multitude of lines it is clear that we are indeed dealing with a delocalized electron of a shallow donor that interacts with a large number (tens) of ^{67}Zn nuclei.

In Fig. 2 the ENDOR spectra of the ^{67}Zn nuclei are presented symmetrically placed around the ^{67}Zn Zeeman frequency at 9.2 MHz for ZnO particles of various radii. The remarkable observations are that the ENDOR band broadens upon size reduction and develops a dip around the Zeeman frequency of the ^{67}Zn nuclear spins. The dip becomes more prominent and broader when the radius of the ZnO core is reduced from r = 3.0 via 1.6 to 1.17 nm. The broadening of the ENDOR band gives evidence that the maximum density of the electronic wave function increases when reducing the size of the QD. The disappearance of the ENDOR signals close to the ^{67}Zn Zeeman frequency, which corresponds to a virtual zero density of the electronic wave function, shows that the density of the envelope wave function at the interface also increases as a result of the confinement. In other words, the dip in the ENDOR spectrum indicates that for the small particles, even at the interface, the Zn nuclei carry non-zero spin density. The appearance of the deep one can consider as an evidence of the collapse of HF interaction with remote Zn shells. This conclusion is in line with our observation that the electronic density at the ZnO/$Zn(OH)_2$ interface, as measured from the linewidth of the ^{1}H ENDOR signal, increases with decreasing size of the particles. It is

interesting to note that estimates of the electronic density at the ZnO/$Zn(OH)_2$ interface, using either the width of the dip in the ^{67}Zn ENDOR signal or the linewidth of the ^{1}H ENDOR signal and using the amplification factors for Zn and H [11], give about the same value (continuity of wave function in quantum theory).

The HF splitting (e.g., for ^{7}Li ENDOR lines) is equal to the isotropic HF interaction of the unpaired electron spin with the nuclear spin of SD and thus proportional to the density of the electronic wave function at the position of the SD core (e.g., Li ion). Thus the observation of the ENDOR signals (e.g., for ^{7}Li) allows to measure directly the effect of confinement on the wave function of the SD. To this end we have measured the dependence of the HF splitting as a function of the QD radius r_{QD} of the ZnO QDs has been measured [8] which is proportional to the density of the electronic wave function at the position of the SD in ZnO crystal core. The SD position is considered to be at or near the centre of the ZnO QD, based on the small size of the hydrogen HF interaction.

It was shown that one can monitor the change of the electronic wave function of a shallow donor in a ZnO QDs when entering the regime of quantum confinement by using the nuclear spins in the semiconductor nanocrystals as probes. The model, based on the effective mass approximation works down to R = 1.5 nm and does not yield an appropriate description of the electronic wave function when the radius of the ZnO nanocrystalline core is reduced below the Bohr radius of ~1.5 nm. Molecular, cluster-type calculations should be carried out to describe the observed behaviour.

One can also see that symmetrically around the Zeeman frequency of ^{7}Li (I=3/2, abundance 92.5 %) at 57.1 MHz two ENDOR lines are present, separated by 90 kHz, that are assigned to ^{7}Li. These signals are taken as proof that Li^{+} forms an interstitial core for the shallow donor electron in the ZnO crystal core of ZnO QDs.

To check whether interstitial Na similar to interstitial Li can also act as a shallow donor in ZnO QDs EPR and ENDOR experiments on ZnO nanoparticles that were treated with NaOH have been performed. Two transitions with a splitting of 300 kHz symmetrically placed around the Zeeman frequency of ^{23}Na at 38.97 MHz have been observed (see Fig. 2) which can be considered as proof of the presence of a shallow donor related to interstitial Na in the ZnO crystal core of ZnO QDs.

It is seen in Fig. 2 that an ENDOR line is present with a width $\Delta\nu$ = 60 kHz exactly at the Zeeman frequency of ^{1}H. From the width we deduce a ^{1}H HF interaction smaller than 60 kHz. This should be compared to observation on the interstitial-hydrogen related shallow donor in a bulk crystal of ZnO where two ENDOR lines were found with a hyperfine splitting of 1.4 MHz (see Fig. 2). The observed ENDOR lines were concluded to originate in the hydrogen atoms present in the $Zn(OH)_2$ capping layer where the density of the electronic wave function is very small.

Fig. 2 shows the ENDOR spectrum of ^{27}Al nuclei as observed in the EPR signal of the shallow donor in ZnO:Al QDs. Two broad ENDOR lines separated symmetrically around the nuclear Zeeman frequency of ^{27}Al (I=5/2, abundance 100%) at 38.4 MHz are seen. This splitting is due to the HF interaction with ^{27}Al and corresponds to the HF interaction constant $A(^{27}Al)$=1.45 MHz. The boxlike form of the ENDOR spectrum is caused by the quadrupole splitting that gives rise to five unresolved lines of the ^{27}Al nuclei. Note, the value of the quadrupole splitting of ^{27}Al is nearly the same as quadrupole splitting for ^{67}Zn nuclear spins in ZnO. Moreover, the nuclear spins and the quadrupole moments of ^{27}Al and ^{67}Zn are the same, too. As a reference, the ENDOR spectrum of the ^{67}Zn nuclei, detected via EPR of the shallow interstitial H donor in ZnO single crystals with $B \perp c$, is shown on the same scale as the ENDOR signals of ^{27}Al in Fig. 2. This indicates that the intrinsic electric-field gradients at the Zn nuclear sites and Al site seem to be virtually the same. This finding is taken to support the assumption that Al enters the ZnO nanocrystals substitutionally and that it is centrally located at the Zn site. Consequently, it may form a core for the shallow donor electron in the ZnO:Al nanocrystal core.

The signals II (Fig. 1) with resolved hyperfine structure of four lines were detected in all the ZnO QDs under investigation. These signals are interpreted as arising from a deep Na-related acceptor localized near interface of ZnO nanocrystalline core and capping layer. The observations leading to this assignment are the following. When heating the sample from 1.6 K to 200 K the EPR signal II gradually disappears simultaneously with signal I of the shallow donor lending support to the idea that the thermally released, donor electron is captured by the Na-related centre. The two signals I, and II remain invisible when the sample is subsequently cooled in the dark to 1.6 K. They reappear when the sample is again irradiated with UV light at 1.6 K. This shows that upon irradiation an electron is transferred from the Na-related impurity to the shallow donor making both centres paramagnetic.

The Na-related acceptor must be located close to or at the ZnO/$Zn(OH)_2$ interface. This conclusion is drawn from the observation that in the EPR signal II not only the ENDOR signals of the ^{23}Na (I=3/2) nucleus can be observed, but also the ENDOR signal of ^{1}H (I=1/2) nuclear spins. Moreover the line width of 1.0 MHz is about 8

times larger than the line width of the ^{1}H ENDOR signals observed in the ESE-detected EPR signal of the shallow donor. This shows that the density of the electronic wave function of the Na-related acceptor is relatively large in the $Zn(OH)_2$ capping layer.

We propose as the most probable structure for the deep Na-related acceptor a Na^+ on a Zn position at the surface of the ZnO core with two OH^- ligands of the $Zn(OH)_2$ capping layer. This structure resembles the Na-related deep acceptor in bulk ZnO consisting of a Na^+ on a Zn position and surrounded by four O^{2-} ligands [12]. Similarly, the deep Na-related acceptor is diamagnetic, negatively charged and capable to capture a hole that most probably will be located on one of the O^{2-} ligands. When irradiating with above-band-gap light an electron of one of the O^{2-} ligands is transferred to the shallow donor making both centres paramagnetic.

The arguments leading to the assignment of signal I*II (see Fig. 1) to the exchange-coupled pair of the shallow donor and the deep Na-acceptor are the following. First its g-value g_p is the average of the g-values g_D of the shallow donor and the g-value g_A of the deep Na-acceptor: $g_p = ½(g_D + g_A)$. This is the g-value that one predicts for an exchange-coupled donor-acceptor pair when the exchange coupling $J >> ½(g_D - g_A)\mu_B B_0$. Here μ_B is the Bohr magneton of the electron and B_0 the strength of the magnetic field. Second, the pair signal is only visible in ZnO nanoparticles with a radius smaller than 1.5 nm, when the distance between the donor and acceptors become smaller than SD Bohr radius $r_B \sim 1.5$ nm. For the larger radius QDs the probability for pair formation is so small that the related EPR signal is no longer observable.

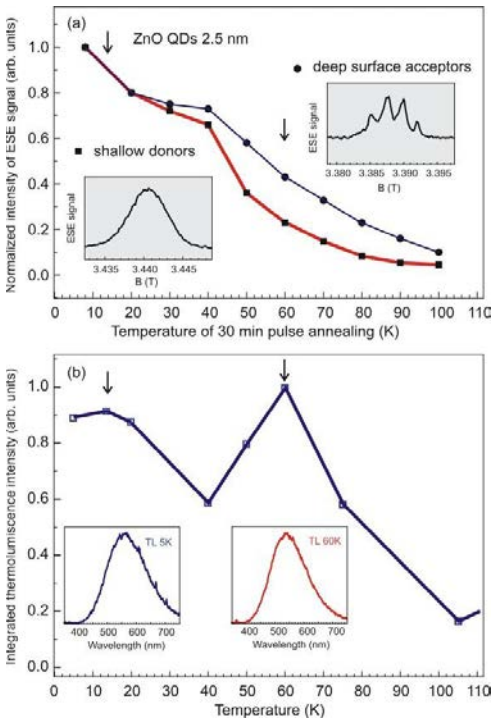

Fig. 3. (a) Dependence of ESE signal intensity at 275 GHz and at 8 K of shallow donor signal I (circles) and deep Na-related surface acceptor signal II (squares) on temperature of pulse annealing (about 30 min at every temperature) normalized to their original 8 K values for Li-doped ZnO QDs with an average radius of 1.3 nm after an anneal at higher temperatures. (b) Integrated thermoluminescence relative intensity (60 s acquisition – CCD) at various temperatures after UV illumination at 320 nm during 2 h at 4.2 K

The recombination of the donors and acceptors as observed in the EPR-detected annealing experiments is accompanied by an intense thermoluminescence (TL). Integrated thermoluminescence relative intensity (60 s acquisition – CCD) at various temperatures after UV illumination at 320 nm during 2 h at 4.2 K is shown in Fig. 3(b).The emission spectra at 5 K (it is attributed to tunneling afterglow since this emission cannot be thermally induced at 5 K) and 60 K (thermoluminescence) are shown in insets.

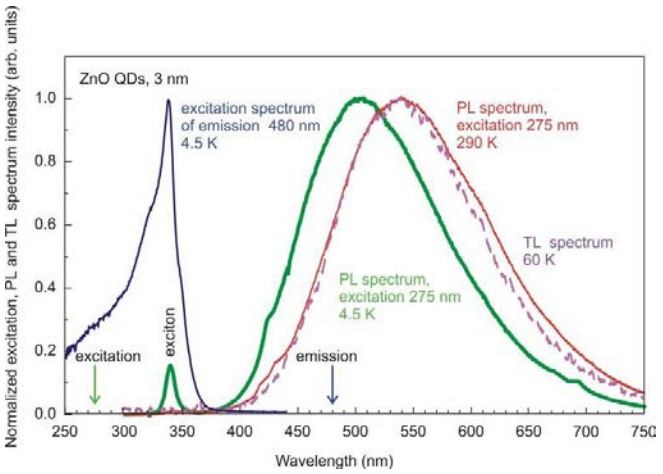

Fig. 4. The photoluminescence excitation spectrum, observed by monitoring emission at 480 nm at 4.5 K and emission spectra at 4.5 K and 290 K excited with wavelength of 275 nm in ZnO QDs, diameter of 2.75 nm. Thermoluminescence spectrum observed at 60 K after UV excitation at 4.5 K with wavelength of 320 nm during 2 hours.

In Fig. 4 the thermoluminescence spectrum observed at 60 K after UV excitation at 4.5 K with wavelength of 320 nm during 2 hours is shown together with the photoluminescence (PL) spectra at 5 K and at 290 K for Li-doped ZnO nanocrystals with an average radius of 1.3 nm. In addition the photoluminescence excitation spectrum, observed by monitoring emission at 480 nm at 4.5 K and emission spectra at 4.5 K and 290 K excited with wavelength of 275 nm in ZnO QDs.

The technique of ODMR detection via tunneling afterglow that can be observed at low temperatures after X-ray or UV irradiation and in some cases persists for a long time after the irradiation proved to be very effective for a study of ZnO QDs. The tunnelling afterglow is determined by the recombination of electron and hole centres that were created during irradiation. The recombination is forbidden for electrons and holes with parallel spins. Therefore, in the magnetic field at a low temperature, when all spins tend to orient along the field as a result of the Boltzmann polarization, the afterglow intensity decreases. Reorientation of the spins of an electron or a hole centre at magnetic resonance results in a strong increase in the afterglow intensity and allows detecting EPR of the recombining centres. The technique is very sensitive and allows using magnetic resonance for characterisation of ZnO nanocrystals not only as a dry powder but also as nanocrystals dispersed in transparent media, which cannot be studied by conventional EPR and ESE. This is an important advantage, since these systems are more relevant for a number of practical applications.

The afterglow-detected ODMR spectrum of not specifically doped ZnO nanocrystals is shown in Fig. 5. Analysis of this spectrum provides direct information on the recombination processes that cause the afterglow and the nature of the recombining centers. Simulation of the ODMR spectrum with the known parameters of different types of deep acceptors in ZnO nanocrystals proves that the afterglow is due to recombination of shallow donors, surface Na acceptors, Zn vacancies and deep Li_{Zn} acceptors.

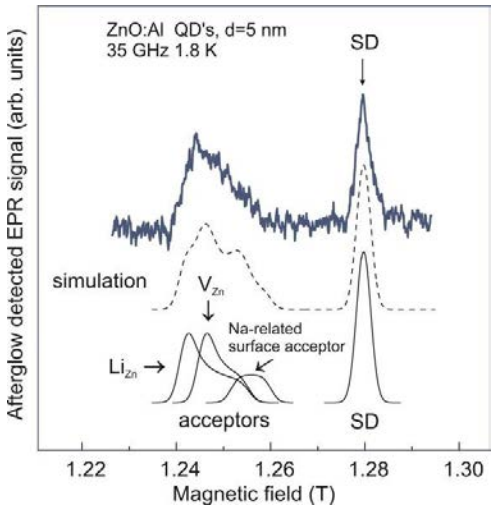

Fig. 5. 35 GHz ODMR spectrum recorded at 1.8 K by monitoring the afterglow intensity ca. 30 min after switching off UV excitation in undoped ZnO QDs with a diameter of 2.5 nm dispersed in ethanol. Baseline is subtracted. Results of simulation of the ODMR spectrum presented in the bottom show that the afterglow is caused by recombination of shallow donors (SD) and several types of deep acceptors.

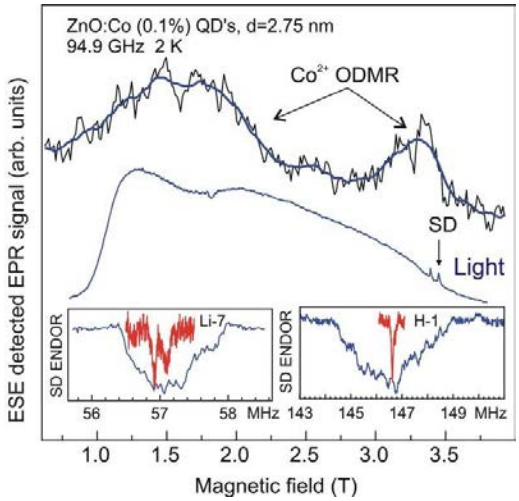

Fig. 6. (a) 94 GHz ESE spectrum of ZnO:Co (0.1%) nanocrystals and ODMR recorded by monitoring the photoluminescence intensity in ZnO:Co (1%) with a diameter of 2.75 nm. Insets in the bottom show ENDOR spectra recorded at EPR of shallow donors in undoped ZnO nanocrystals (upper curves) and in nanocrystals of ZnO:Co (0.1%) (lower curves).

94 GHz EPR, ESE and ENDOR at 94.9 GHz were applied to study of Co- and Mn- doped ZnO QDs which consist of a $ZnO/Zn(OH)_2$ core-shell structure. The ESE and ENDOR spectra of 2.75 nm nanocrystals with a diameter of 2.75 nm are shown in Fig. 3 together with the ODMR spectrum of ZnO:Co (1%) nanocrystals recorded via photoluminescence intensity. The shape of the EPR spectrum of cobalt ions changed as a result of Co^{2+} coupling with optically created shallow donors. The introduction of shallow donors in a quantum dot with a low concentration of cobalt was shown to change the shape of the EPR spectrum and results in virtually identical EPR spectra of cobalt ions in the quantum dots with higher concentration of cobalt. That is to say that the introduction of SDs raises interaction between cobalt ions, apparently due to an indirect interaction through the shallow donor, the wave function which almost fills the entire space of the quantum dot. This, along with a shift of SDs line, is a direct

demonstration of interaction between the magnetic ion and donor electron in confined system of ZnO QD. This interaction is the reason of a broadening of the ENDOR spectra of shallow donors. ENDOR resonance of the ^{1}H hydrogen nuclei registered by the EPR signal of Co^{2+} and Mn^{2+} evidence the hyperfine coupling between these ions, located in the ZnO core, and the protons outside the quantum dot core in the $Zn(OH)_2$ shell.

4. Conclusions

In colloidal ZnO QDs hyperfine interactions as monitored by ENDOR quantitatively reveal the transition from semiconductor to molecular properties upon reduction of the size of the nanoparticles. We studied the process of charge separation in the quantum dot when excited by UV light resulting in the formation of shallow donors and deep acceptors in the paramagnetic state, which recombine when heated, accompanied by thermoluminescence go back again in the non-paramagnetic state. It was shown that in all studied quantum dots deep acceptors are present positioned near the interface and including one sodium atom. ODMR techniques, which is based on EPR detection via photoluminescence or via tunneling afterglow that can be observed after preliminary X-ray or UV irradiation proved to be very useful to study colloidal ZnO NCs. The higher sensitivity of ODMR via afterglow allowed characterization of ZnO QDs dispersed in transparent media, which is an important advantage, since these systems are more relevant for a number of practical applications. A direct evidence of Co (Mn) interaction with SD in the core and hyperfine coupling with 1H in the shell of QDs has been demonstrated in Mn (Co)-doped ZnO QDs, which are promising classes of diluted magnetic semiconductors.

Acknowledgements

The work has been supported by Russian Science Foundation under Agreement № 14-12-00859.

References

[1] A.Janotti and C. G. Van de Walle, Rep. Prog. Phys. 72 (2009) 126501.
[2] Ü. Ozgür, Y.I. Alivov, C. Liu, A. Teke, M.A. Reshchikov, S. Dogan, V.Avrutin, S.-J. Cho and H.J. Morkoc¸ Appl. Phys. 98 (2005) 041301.
[3] K.R. Kittilstved, W.K. Liu, D.R. Gamelin, Nature material, 5 (2006) 291-297.
[4] M. Nirmal, B.O. Dabbousi, M.G.Bawendi, J.J. Macklin, J.K. Trautman, T.D.Harris, and L.E. Brus, Nature 383, 802-804 (1996).
[5] A.L. Efros, and M. Rosen, Phys. Rev. Lett., 78 (1997) 1110-1113.
[6] R.Verberk, A. van Oijen, and M. Orrit, Phys. Rev. B 66, 233202 (2002).
[7] P.G. Baranov, S.B. Orlinskii, C. de Mello Donegá, J. Schmidt, Appl. Magn. Reson., 39 (2010) 151–183.
[8] E. A. Meulenkamp, J. Phys. Chem. B 102 (1998) 5566-5572.
[9] NANOPARTICLES: Workhorses of Nanoscience, ed. C. de Mello Donega, Springer, Heidelberg- New York- Dordrecht-London, 2014.
[10] S.B. Orlinskii, J. Schmidt, P.G. Baranov, V. Lorrmann, I. Riedel, D. Rauh, and V.V. Dyakonov, Phys. Rev. B 77 (2008) 115334.
[11] D.M. Hofmann, A.Hofstaetter, F. Leiter, H. Zhou, F. Henecker, B.K. Meyer, S.B. Orlinskii, J. Schmidt, and P.G. Baranov, Phys. Rev. Lett. 88 045504 (2002).
[12] O.F. Schirmer, and D. Zwingel, Solid State Commun. 8 (1970) 1559-1563.